Cell Reports, Volume *14*

Supplemental Information

The Oxygen Sensor PHD2 Controls Dendritic Spines and Synapses via Modification of Filamin A

Inmaculada Segura, Christian Lange, Ellen Knevels, Anastasiya Moskalyuk, Rocco Pulizzi, Guy Eelen, Thibault Chaze, Cicerone Tudor, Cyril Boulegue, Matthew Holt, Dirk Daelemans, Mariette Matondo, Bart Ghesquière, Michele Giugliano, Carmen Ruiz de Almodovar, Mieke Dewerchin, and Peter Carmeliet

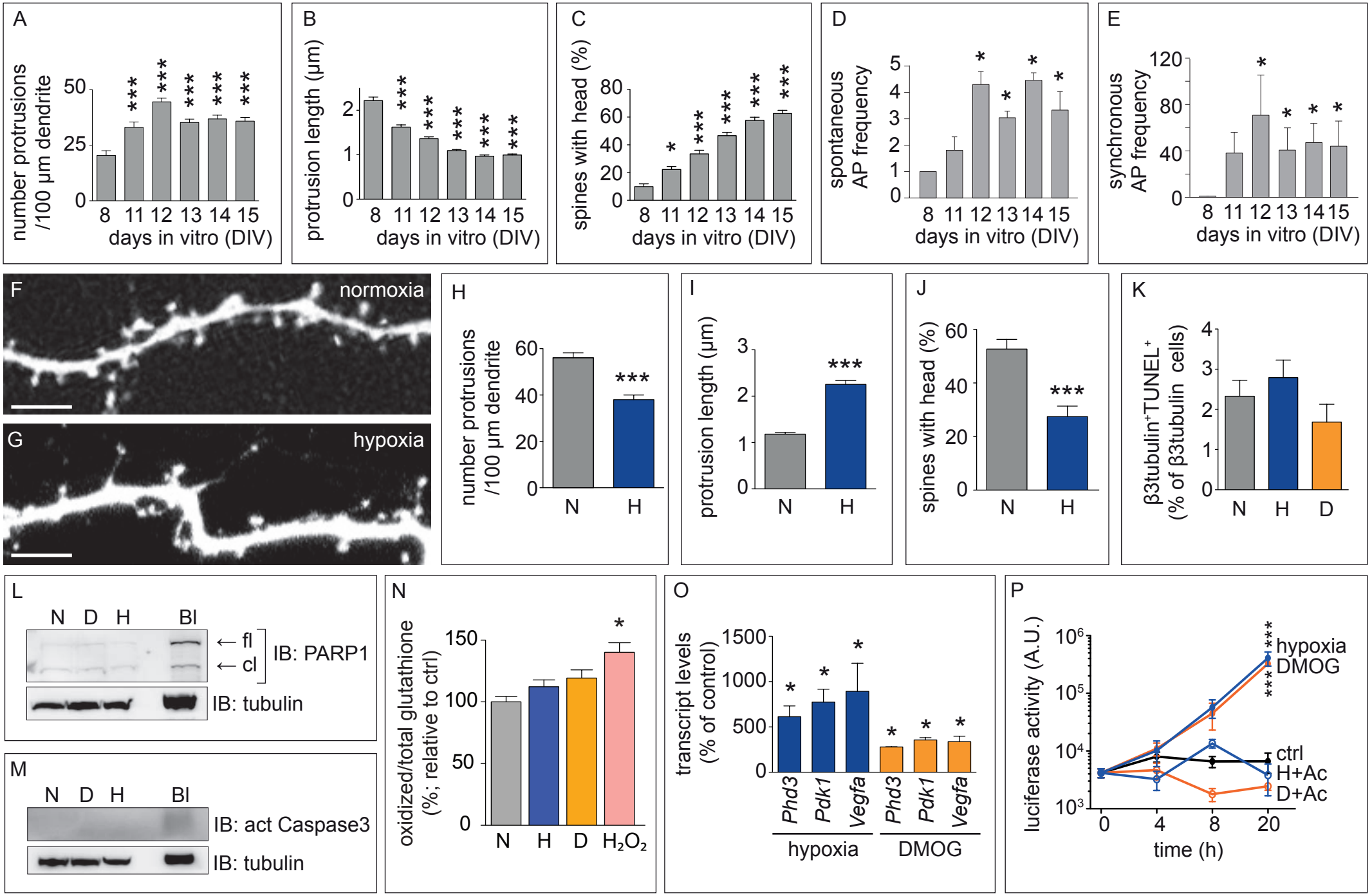
A
number protrusions /100 µm dendrite
50
25
0
***
8 11 12 13 14 15
days in vitro (DIV)
B
protrusion length (µm)
2
1
0
***
8 11 12 13 14 15
days in vitro (DIV)
C
spines with head (%)
80
60
40
20
0
*
***
8 11 12 13 14 15
days in vitro (DIV)
D
spontaneous AP frequency
5
4
3
2
1
0
*
8 11 12 13 14 15
days in vitro (DIV)
E
synchronous AP frequency
120
80
40
0
*
8 11 12 13 14 15
days in vitro (DIV)
F
normoxia
G
hypoxia
H
number protrusions /100 µm dendrite
60
40
20
0
***
N H
I
protrusion length (µm)
3
2
1
0
***
N H
J
spines with head (%)
60
40
20
0
***
N H
K
β3tubulin+TUNEL+ (% of β3tubulin cells)
4
3
2
1
0
N H D
L
N D H BI
← fl
← cl
IB: PARP1
IB: tubulin
M
N D H BI
IB: act Caspase3
IB: tubulin
N
oxidized/total glutathione (%; relative to ctrl)
150
100
50
0
*
N H D H2O2
O
transcript levels (% of control)
1500
1000
500
0
*
Phd3 Pdk1 Vegfa Phd3 Pdk1 Vegfa
hypoxia
DMOG
P
luciferase activity (A.U.)
10^6
10^5
10^4
10^3
****
hypoxia
DMOG
ctrl
H+Ac
D+Ac
0 4 8 20
time (h)

FIGURE S1

FIGURE S1; RELATED TO FIGURE 1

In all panels, N: normoxia, H: hypoxia (1% O_2), D: DMOG (250 μM). **A-C,** Time course analysis of dendritic spines in MHNs in vitro. Protrusion density (A), protrusion length (B), and percentage of spines with head (C) was evaluated in tdT labeled dendrites of MHNs at the indicated DIVs (n = 3 experiments, 30 neurons, 30-60 dendrites, 294-762 protrusions). **D,E,** Frequency of spontaneous action potential (AP) firing (D) and network-wide AP synchronization in vitro (E) at the indicated DIVs (n = 4 multi-electrode arrays (MEAs)). Data are normalized to the activity at 8 DIV. **F-J,** tdT-transfected 21 DIV MHNs in control (normoxia) conditions (F) or after 20 DIV in control conditions plus an additional 16 hr in hypoxia (G), and analyzed for protrusion density (H), protrusion length (I) and percentage of spines with head (J) ($n \geq 7$ neurons, 12 dendrites, 350-500 protrusions). **K,** Quantification of apoptotic ($TUNEL^+$) 14 DIV MHNs after control, hypoxia or DMOG treatment for 16 hr. **L,** Representative immunoblot (IB) for PARP1 and tubulin in lysates from 14 DIV MHN after control (normoxia), DMOG or hypoxia treatment for 16 hr. Brain lysate (Bl) was used as positive control. Arrows indicate full-length (fl) or cleaved (cl) PARP1. **M,** Representative IB for active (act) caspase3 and tubulin in lysates from 14 DIV MHN after control (normoxia), DMOG or hypoxia treatment for 16 hr. Brain lysate (Bl) was used as positive control. **N**, Content of oxidized glutathione (GSSG) vs. total glutathione (GSSG + GSH) (expressed in % of the value in normoxia) in 14 DIV MHNs in control normoxic conditions, hypoxia or DMOG treatment for 16 hr. MHNs treated with 100 μM H_2O_2 for 1 hr were used as a positive control (H_2O_2). **O,** RT-PCR expression analysis of hypoxia-responsive genes in MHNs exposed to hypoxia or treated with DMOG for 16 hr (expressed in % of normoxia control; n = 3 experiments). *Phd3*, prolyl hydroxylase domain 3; *Pdk1*, pyruvate dehydrogenase kinase 1; *Vegfa*, vascular endothelial growth factor A. **P,** Quantification of luciferase activity from MHNs transfected with the HIF-dependent luciferase reporter HRE::luc plasmid and incubated for the indicated time points in control (ctrl) conditions, DMOG (D) treatment or hypoxia (H) alone or combined with the HIF-inhibitor acriflavine (Ac). A.U., arbitrary units. Data are mean ± SEM. *$p < 0.05$, ***$p < 0.001$. Scale bar, 5 μm (F,G).

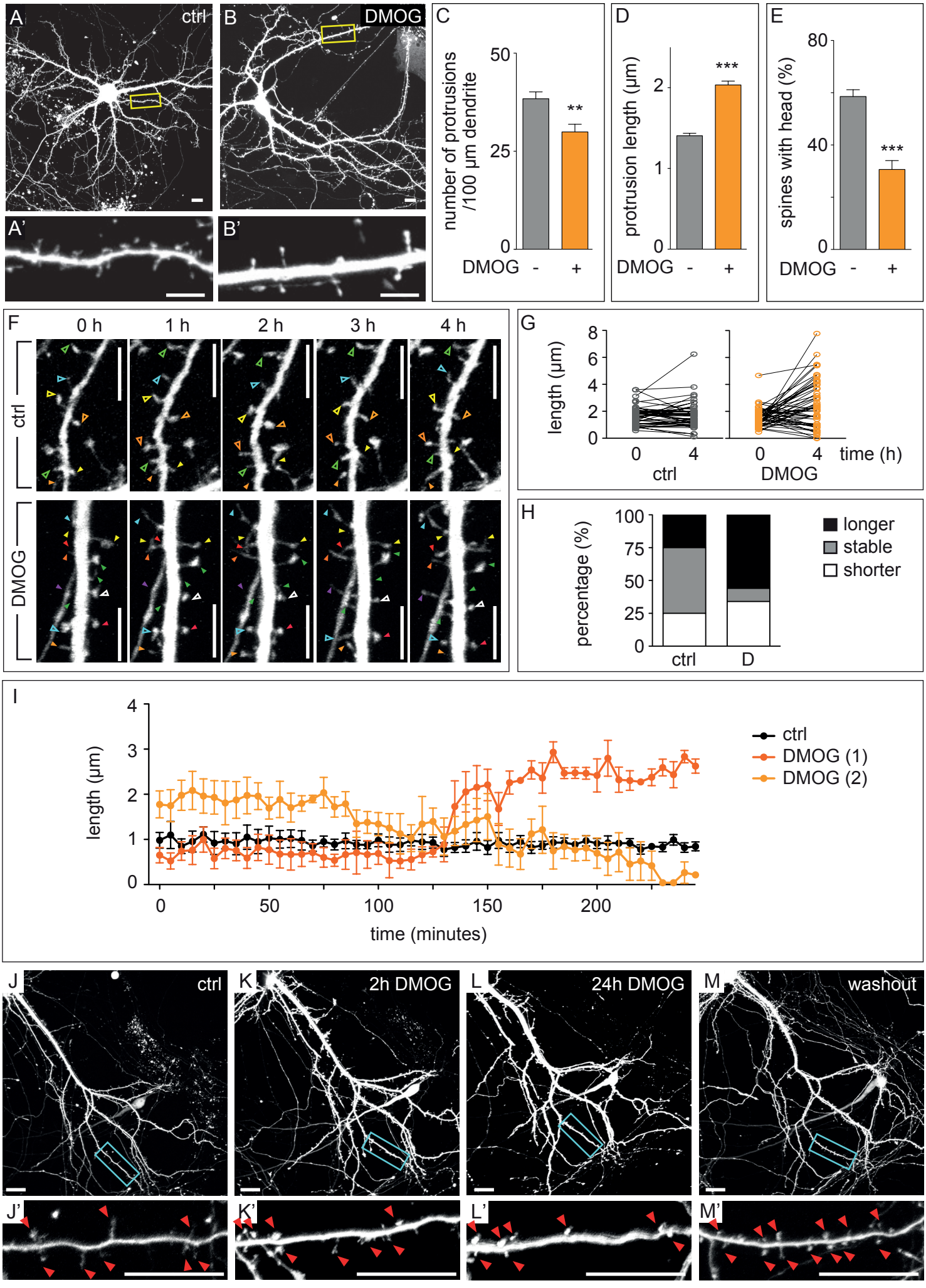
A
ctrl
B
DMOG
A'
B'
C
number of protrusions /100 µm dendrite
50
25
0
**
DMOG - +
D
protrusion length (µm)
2
1
0
***
DMOG - +
E
spines with head (%)
80
40
0
***
DMOG - +
F
0 h
1 h
2 h
3 h
4 h
ctrl
DMOG
G
length (µm)
8
6
4
2
0
0 4
ctrl
0 4
DMOG
time (h)
H
percentage (%)
100
75
50
25
0
ctrl
D
longer
stable
shorter
I
length (µm)
4
3
2
1
0
0
50
100
150
200
time (minutes)
ctrl
DMOG (1)
DMOG (2)
J
ctrl
K
2h DMOG
L
24h DMOG
M
washout
J'
K'
L'
M'

FIGURE S2

FIGURE S2; RELATED TO FIGURE 1

A-E, YFP-transfected MHNs were incubated for 16 hr under control (A) or 250 μM DMOG (B) and analyzed for protrusion density (C), protrusion length (D) and percentage of spines with head (E) (n = 3 experiments, ≥ 21 neurons, > 550 protrusions). A'-B' show higher magnifications of the box in A or B. **F**, Snap-shot images at the start (0) and after 1, 2, 3 or 4 hr of time-lapse recording of 14 DIV tdT-labeled MHNs, in control (upper) or DMOG conditions (lower). Solid arrowheads: spines with persistent increase or decrease in length; open arrowheads: spines that do not change their length. Each color denotes a distinct spine. **G,H**, Length of single protrusions at 0 and 4 hr recording for control and DMOG (G; n ≥ 40) and distribution of spines according to length variation (H). Stable: Δ-length ≤ 0.2 μm..**I,** Diagram showing the average length of randomly selected control (black) and DMOG-treated (orange) dendritic spines over time, showing different subpopulations responding to the treatment by reducing (light orange) or increasing (dark orange) their length; n = 5 spines per condition; representative of 3 experiments. **J-M',** Representative pictures of the same tdT transfected MHN taken at 13 DIV before treatment (J,J'), at 14 DIV after DMOG treatment for 2 hr (K,K'), at 15 DIV after DMOG treatment for 24 hr (L,L'), and at 18 DIV after washout for 3 DIV (M,M'). J'-M' show higher magnification of the boxed areas in J-M; red arrowheads: dendritic protrusions. Data are mean ± SEM. **p < 0.01, ***p < 0.001. Scale bar, 5 μm (A',B',F), 10 μm (A,B), 20 μm (J, J'-M, M').

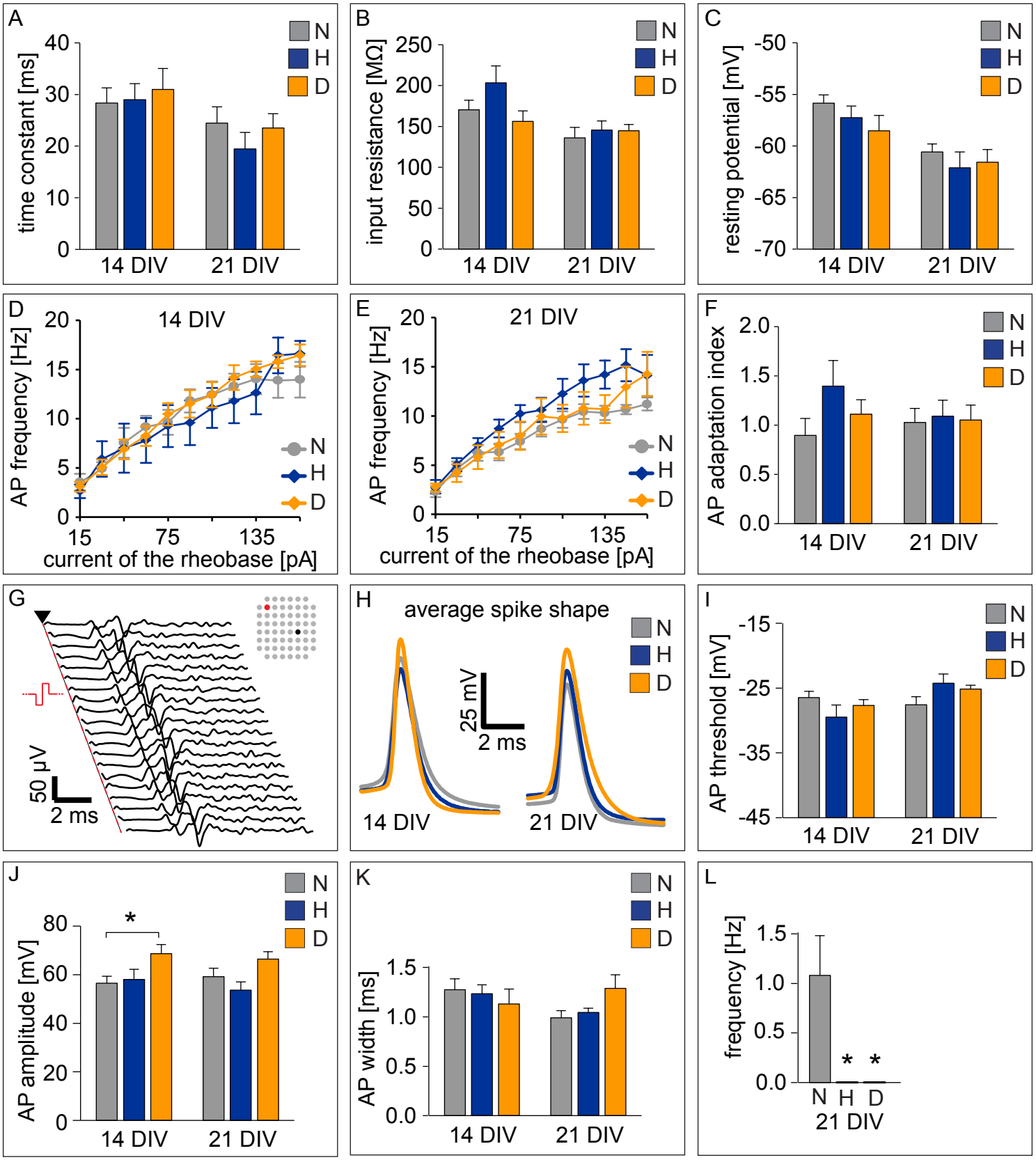
A
time constant [ms]
40
30
20
10
0
14 DIV
21 DIV
N
H
D
B
input resistance [MΩ]
250
200
150
100
50
0
C
resting potential [mV]
-50
-55
-60
-65
-70
D
14 DIV
AP frequency [Hz]
20
15
10
5
0
15
75
135
current of the rheobase [pA]
E
21 DIV
F
AP adaptation index
2.0
1.5
1.0
0.5
0.0
G
50 µV
2 ms
H
average spike shape
25 mV
2 ms
I
AP threshold [mV]
-15
-25
-35
-45
J
AP amplitude [mV]
80
60
40
20
0
*
K
AP width [ms]
1.5
1.0
0.5
0.0
L
frequency [Hz]
1.5
1.0
0.5
0.0
* *
N H D
21 DIV

FIGURE S3

FIGURE S3; RELATED TO FIGURE 2

In all panels, N: normoxia, H, hypoxia (1% O_2), D: DMOG (250 μM (A-F,H-L) or 1 mM (N,O)), H/N: hypoxia o/n followed by 24 hr normoxia. **A-C,** Single-neuron passive electrical properties of 14 and 21 DIV MHNs, measured by patch-clamp at the soma (n = 30 neurons) and quantification of the membrane time constant (A), apparent input resistance (B), and membrane resting potential (C). **D-F,** Excitable, active electrical neuronal properties (n = 30 neurons) of 14 (D,F) and 21 DIV (E,F) MHNs, studied by the relationship between current amplitude of the rheobase and the mean frequency of evoked action potential (AP; D,E), and by the temporal adaptation of successive APs in a train (F). **G**, Antidromic APs could be elicited with no failures during hypoxia by 20 repeated extracellular electrical pulses (monopolar configuration, biphasic waves, 1 ms x 800 mV, negative phase first) delivered via substrate-integrated multi-electrode arrays (MEAs). The inset sketches the MEA layout, with the stimulating microelectrode in red, and the recording microelectrode in black. The resulting traces were comparable to those obtained in normoxia (not shown) in their "all-or-none" quality, directly arising from the unaltered cellular and axonal excitability (see also panels D,E). **H**, Average spike shape of spontaneous APs, after recording non stop for 5 minutes and averaging all APs fired, in 14 or 21 DIV MHNs in the indicated conditions. **I-K**, Typical AP features of 14 and 21 DIV MHNs, including threshold (i.e., calculated as the first maximum of the third derivative of the membrane voltage during an AP; I), peak amplitude (J), and width (K). **L**, Spontaneous AP firing as recorded intracellularly by patch-clamp in 21 DIV MHNs, in the indicated conditions, shown as average frequency. **M**, Representative raster plots of the spiking activity, detected in the same neuronal culture by a MEA of 60 extracellular microelectrodes, in normoxia, during hypoxia (after overnight treatment), and 24 hr after return to normoxia. The spontaneous occurrence of one or more action potentials, detected at each of the 60 distinct microelectrode locations, is indicated by a black dot: prominent episodic synchronization is apparent from the vertical structures (i.e., bursts) in the plots and indirectly indicates functional glutamatergic synaptic transmission. **N,O**, Frequency of spontaneous AP firing (N) and spontaneous network-wide AP synchronization (O) (n = 4 MEAs/condition), for the indicated DIV and condition. **P-S,** MHN at 14 DIV transfected with YFP (green) and subjected at 20 DIV for 16 hr to normoxia (P), hypoxia (Q) or 250 μM DMOG (R), fixed and stained for presynaptic synaptophysin (red). The red dots lying outside of the YFP^+ neuron are from neighbouring neurons. Quantification of synaptic density per dendritic length (by counting the yellow clusters and the red clusters in immediate apposition with the dendrite/spine) is shown in S ($n \geq 10$ neurons). Data are mean ± SEM. *$p < 0.05$, **$p < 0.01$, ***$p < 0.001$ (vs. normoxia ctrl).

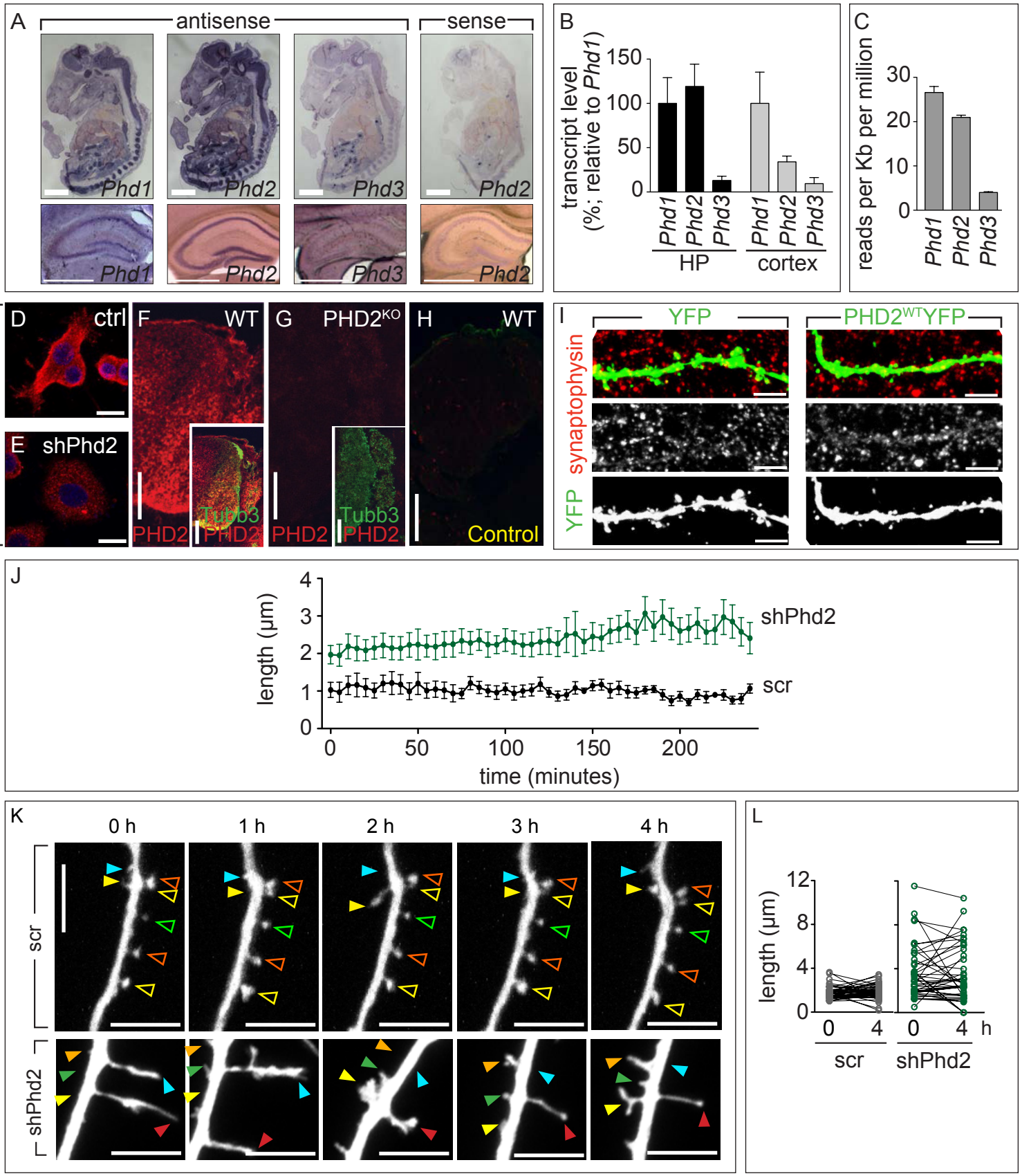
A
antisense
sense
Phd1
Phd2
Phd3
Phd2
Phd1
Phd2
Phd3
Phd2
B
transcript level
(%; relative to Phd1)
150
100
50
0
Phd1
Phd2
Phd3
Phd1
Phd2
Phd3
HP
cortex
C
reads per Kb per million
30
20
10
0
Phd1
Phd2
Phd3
PHD2
DAPI
D
ctrl
E
shPhd2
F
WT
Tubb3
PHD2
PHD2
G
PHD2KO
Tubb3
PHD2
PHD2
H
WT
Control
I
YFP
PHD2WTYFP
synaptophysin
YFP
J
length (µm)
4
3
2
1
0
shPhd2
scr
0
50
100
150
200
time (minutes)
K
0 h
1 h
2 h
3 h
4 h
scr
shPhd2
L
length (µm)
12
8
4
0
0
4
0
4
h
scr
shPhd2

FIGURE S4

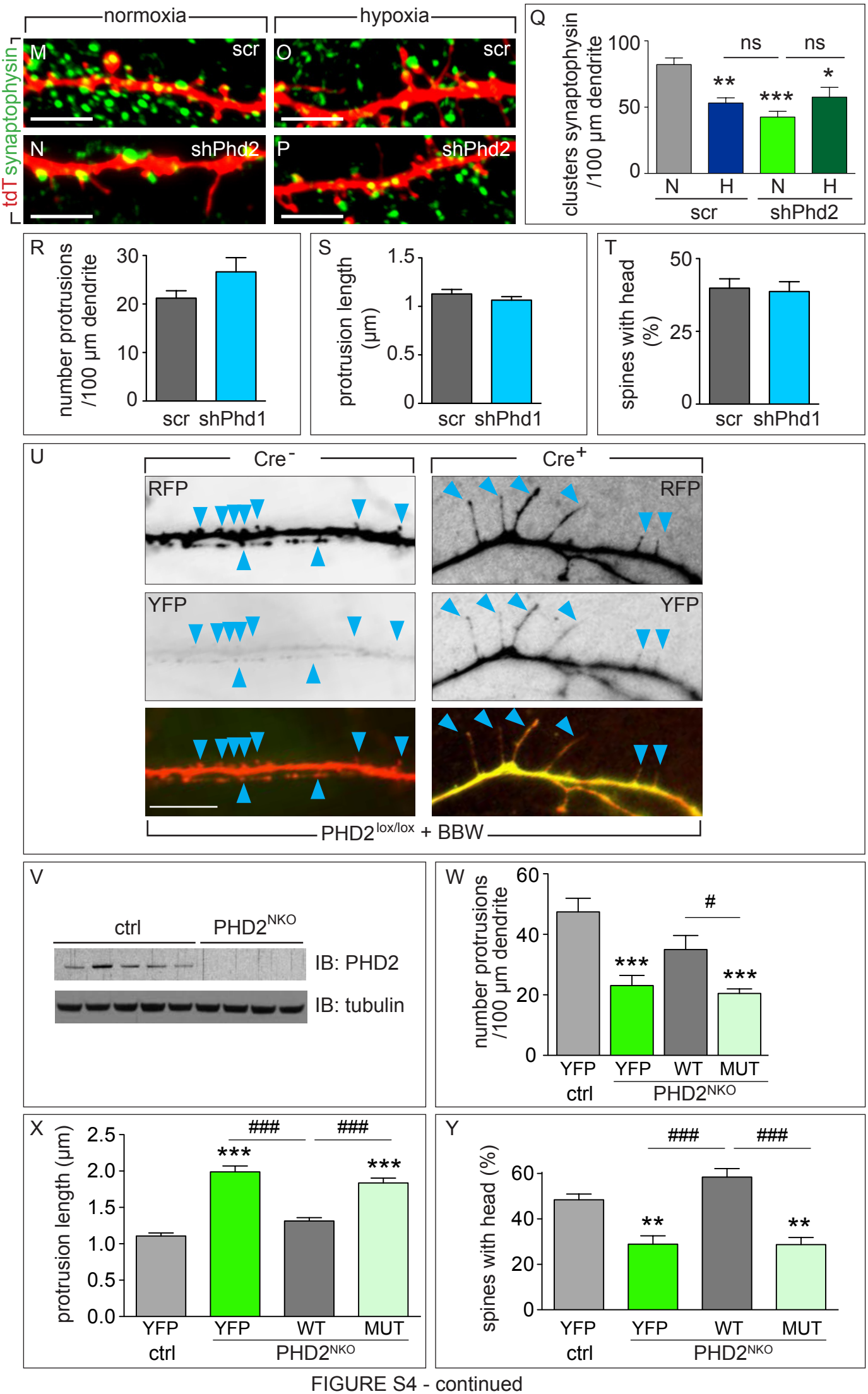

FIGURE S4 - continued

FIGURE S4; RELATED TO FIGURE 3

A, *In situ* hybridization with *Phd1 (also known as Egln2)*, *Phd2 (Egln1)* and *Phd3 (Egln3)* antisense probes or *Phd2* sense probe, in cryosections from E14.5 mouse embryos (upper panels) or in free-floating adult hippocampal coronal sections (lower panels). **B,** Relative mRNA expression of *Phd1*, *Phd2* and *Phd3* genes in E17 hippocampus (HP) and E14.5 cortex (n = 3 embryos). **C,** Quantitative mRNA expression of *Phd1*, *Phd2* and *Phd3* genes in 2 weeks old mouse brains by RNA-seq analysis (n = 3 mice). **D,E,** PC12 cells in control conditions (ctrl, D) or upon silencing of *Phd2* (shPhd2, E) and immunostained for PHD2 (red) and DAPI (blue), showing only negligible (background) staining upon *Phd2* silencing. **F-H,** Immunostaining for PHD2 (red) in cryosections from the trunk of E11.5 control (F) or $PHD2^{KO}$ littermates (G). Small insets show co-staining with the neuronal marker ßIII-tubulin (Tubb3, green). Control staining without both primary antibodies (H). **I,** Representative images of MHNs transfected with YFP or $PHD2^{WT}$YFP expression constructs (green in top panels; white in lower panels) and immunostained for synaptophysin (red in top panels; grayscale in middle panels), showing the expression pattern of $PHD2^{WT}$YFP in neurons in culture, including its presence in postsynaptic sites. The red dots lying outside of the YFP^+ neuron are from neighbouring neurons. **J,** Diagram showing the average length of 5 representative scr (black) or shPhd2 (green) dendritic spines over time; representative of 3 experiments. **K,** Snap-shot images at the start (0) and after 1, 2, 3 or 4 hr of time-lapse recording in normoxia of 14 DIV MHNs co-transfected with YFP or EGFP plus scrambled control shRNA (scr, upper panels) or shPhd2 (lower panels),. Solid arrowheads: spines with persistent increase or decrease in length (longer or shorter at 4 hr, as compared to the start); open arrowheads: spines that do not change their length. Each color denotes a distinct spine. **L,** Length of single protrusions at 0 and 4 hr recording for control and *Phd2* silenced neurons; $n \geq 45$ spines. **M-Q,** MHNs were co-transfected at 14 DIV with tdT (red) and with either scr (M,O) or shPhd2 (N,P), subjected at 20 DIV for 16 hr to normoxia (M,N) or hypoxia (1% O_2, O,P) and stained for synaptophysin (green). The green dots lying outside of the tdT^+ neuron are from neighbouring neurons. Quantification of synaptic density per dendritic length (yellow clusters and green clusters in immediate apposition with the dendrite/spine) is shown in panel Q (n = 8-14 neurons). **R-T,** Quantification of protrusion density (R), protrusion length (S) and percentage of spines with head (T) of MHNs transfected with scr or shPhd1 ($n \geq 10$ neurons, 14-15 dendrites, >200 protrusions). **U,** MHNs isolated from $Phd2^{lox/lox}$ E16.5 embryos were transfected with the Brainbow1.0 plasmid (BBW) alone (Cre^-) or combined with a Cre-recombinase expressing plasmid (Cre^+) at 7 DIV, and imaged at 14 DIV. Note that the Cre^- MHN expresses only RFP, while the Cre^+ MHN expresses YFP and residual RFP. Arrowheads: dendritic protrusions. **V,** Representative IB for PHD2 and tubulin of homogenates obtained from the hippocampus of control (ctrl) and $PHD2^{NKO}$ littermates. **W-Y,** Quantification of protrusion density (W), protrusion length (X) and percentage of spines with head (Y) of 14 DIV MHN isolated from ctrl or $PHD2^{NKO}$ littermates upon transfection at 7 DIV with YFP, $PHD2^{WT}$YFP (WT) or $PHD2^{MUT}$YFP (MUT)). Corresponding representative images are shown in Fig. 3S (n = 7-15 neurons, 203-335 protrusions). Data are mean ± SEM; ns = not significant, $*p < 0.05$, $**p < 0.01$, $***p < 0.001$ vs. scr control in normoxia (Q) or vs. ctr (W-Y); $\#p < 0.01$, $\#\#\#p < 0.001$ between indicated bars. Scale bar: 10 μm (D,E), 5 μm (I,K,M-P,U), 100 μm (F-H), 2000 μm (A).

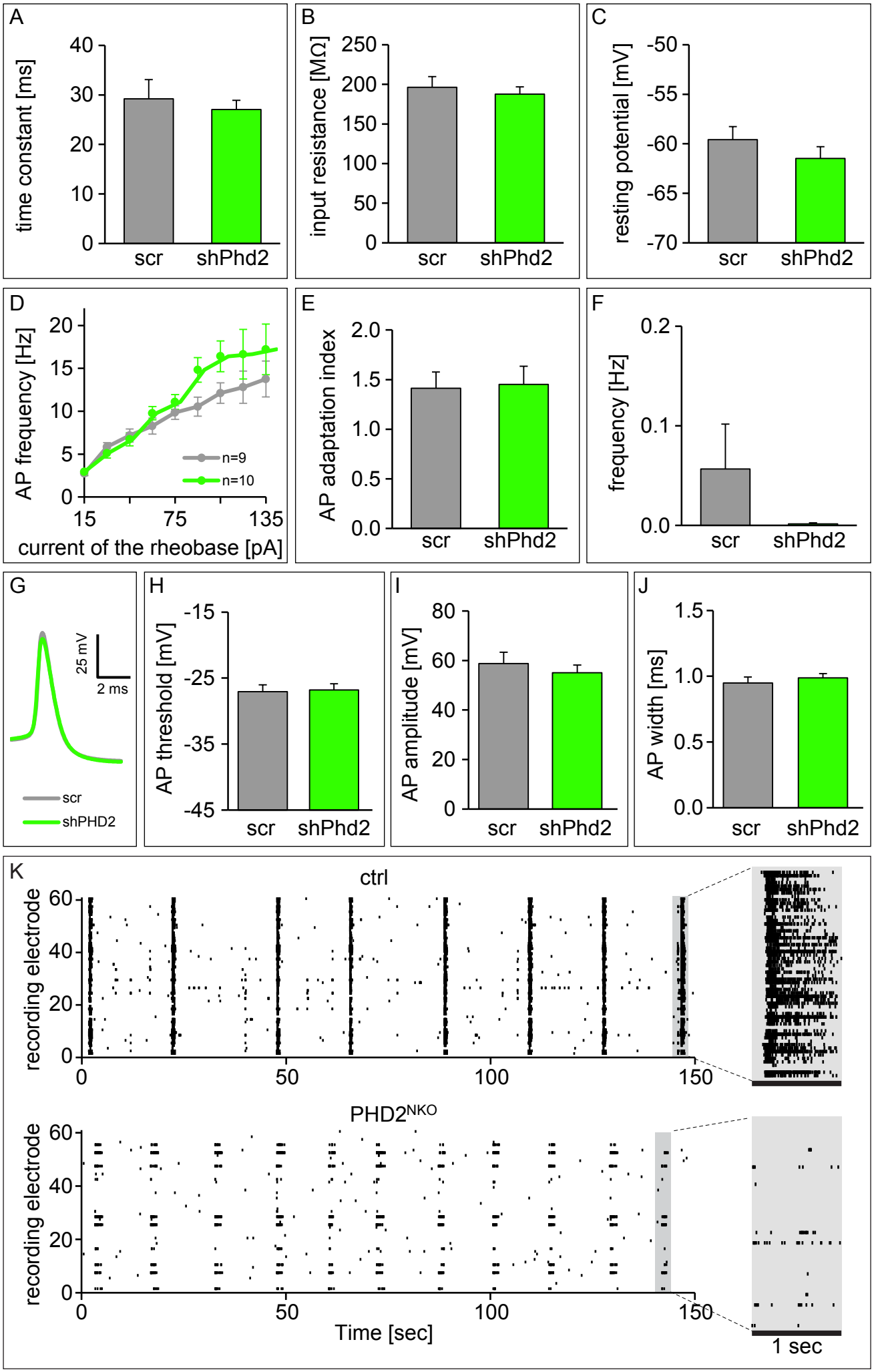
A
time constant [ms]
40
30
20
10
0
scr
shPhd2
B
input resistance [MΩ]
250
200
150
100
50
0
scr
shPhd2
C
resting potential [mV]
-50
-55
-60
-65
-70
scr
shPhd2
D
AP frequency [Hz]
20
15
10
5
0
n=9
n=10
15
75
135
current of the rheobase [pA]
E
AP adaptation index
2.0
1.5
1.0
0.5
0.0
scr
shPhd2
F
frequency [Hz]
0.2
0.1
0.0
scr
shPhd2
G
25 mV
2 ms
scr
shPHD2
H
AP threshold [mV]
-15
-25
-35
-45
scr
shPhd2
I
AP amplitude [mV]
80
60
40
20
0
scr
shPhd2
J
AP width [ms]
1.5
1.0
0.5
0.0
scr
shPhd2
K
ctrl
recording electrode
60
40
20
0
0
50
100
150
PHD2NKO
recording electrode
60
40
20
0
0
50
100
150
Time [sec]
1 sec

FIGURE S5

FIGURE S5; RELATED TO FIGURE 3

A-C, Single-cell passive membrane properties (membrane time constant (A), input resistance (B) and membrane resting potential (C)) measured from soma using patch-clamp recordings in MHNs transduced with lentiviral vectors expressing scrambled (scr) or shPhd2 (n = 27 neurons). **D,E,** Active electrical neuronal properties estimated by mean frequency of evoked action potential in response to current steps with increasing amplitude (D) and time adaptation of action potentials (E) in MHNs transduced with lentiviral vectors expressing scr or shPhd2 (n = 9-10 neurons). **F,** Network properties characterized by the frequency of spontaneous action potentials in MHNs transduced with lentiviral vectors expressing scr or shPhd2 (n = 9-10 neurons). **G-J,** Single action potential properties represented by average shape of action potentials (G), threshold (H), amplitude (I) and width (J), in MHNs transduced with lentiviral vectors expressing scr or shPhd2 (n = 9-10 neurons in H-J). **K**, Representative raster plots of the spiking activity at 14 DIV, detected in two multi-electrode arrays (MEAs) each obtained from a set of control (top) or $PHD2^{NKO}$ neurons (bottom). The spontaneous occurrence of action potentials detected by each of the 60 distinct microelectrodes is indicated by a black dot. Prominent episodic synchronization is apparent in control but not in $PHD2^{NKO}$ cultures. The insets highlight the differences in the firing of the two neuronal networks at higher temporal resolution. Data are mean ± SEM.

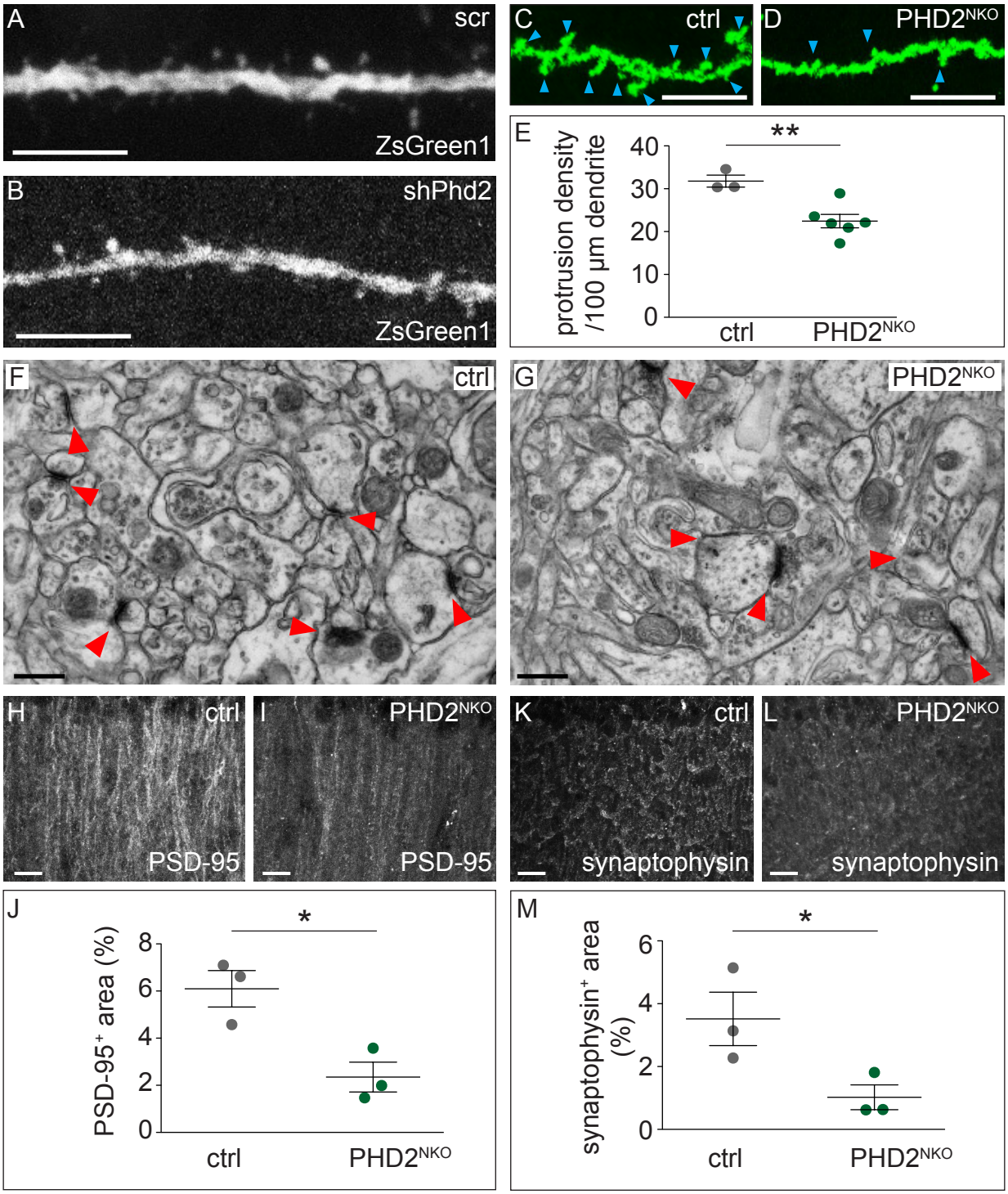
A
scr
ZsGreen1
B
shPhd2
ZsGreen1
C
ctrl
D
PHD2NKO
E
protrusion density /100 µm dendrite
40
30
20
10
0
**
ctrl
PHD2NKO
F
ctrl
G
PHD2NKO
H
ctrl
PSD-95
I
PHD2NKO
PSD-95
K
ctrl
synaptophysin
L
PHD2NKO
synaptophysin
J
PSD-95+ area (%)
8
6
4
2
0
*
ctrl
PHD2NKO
M
synaptophysin+ area (%)
6
4
2
0
*
ctrl
PHD2NKO

FIGURE S6

FIGURE S6; RELATED TO FIGURE 3

A,B, Representative ZsGreen1^{+} dendritic segments from the CA1 region of hippocampal slices of 2-weeks old WT mice that were *in utero* electroporated at E15.5 with a scrambled control shRNA (scr) (A) or shPhd2 (B). **C-E,** Representative dendritic segments from hippocampi of 2 weeks old control (ctrl; C) or PHD2^{NKO} (D) mice, detected by using the Golgi impregnation imaged under the reflection mode of the microscope. Arrowheads: dendritic spines. Panel E shows the quantification of the dendritic protrusion density (n = 3-6 animals). **F,G,** Representative images of the *stratum radiatum* of the CA1 hippocampal region of ctrl (F) or PHD2^{NKO} (G) mice obtained by transmission electron microscopy. Red arrowheads: post-synaptic densities (n = 3-4 animals). **H-M,** Representative images of anti-PSD-95 staining (H,I) and anti-synaptophysin staining (K,L) of the *stratum radiatum* of the CA1 hippocampal region of control (ctrl; H,K) or PHD2^{NKO} (I,L) mice. Quantification of PSD-95^{+} area (panel J; n = 3) and synaptophysin^{+} area (panel M; n = 3) (after setting a common intensity threshold). Single data plus mean ± SEM are shown. *$p < 0.05$, **$p < 0.01$. Scale bar, 5 μm (A,B), 10 μm (C,D), 500 nm (F,G), 20 μm (H,I,.K,L).

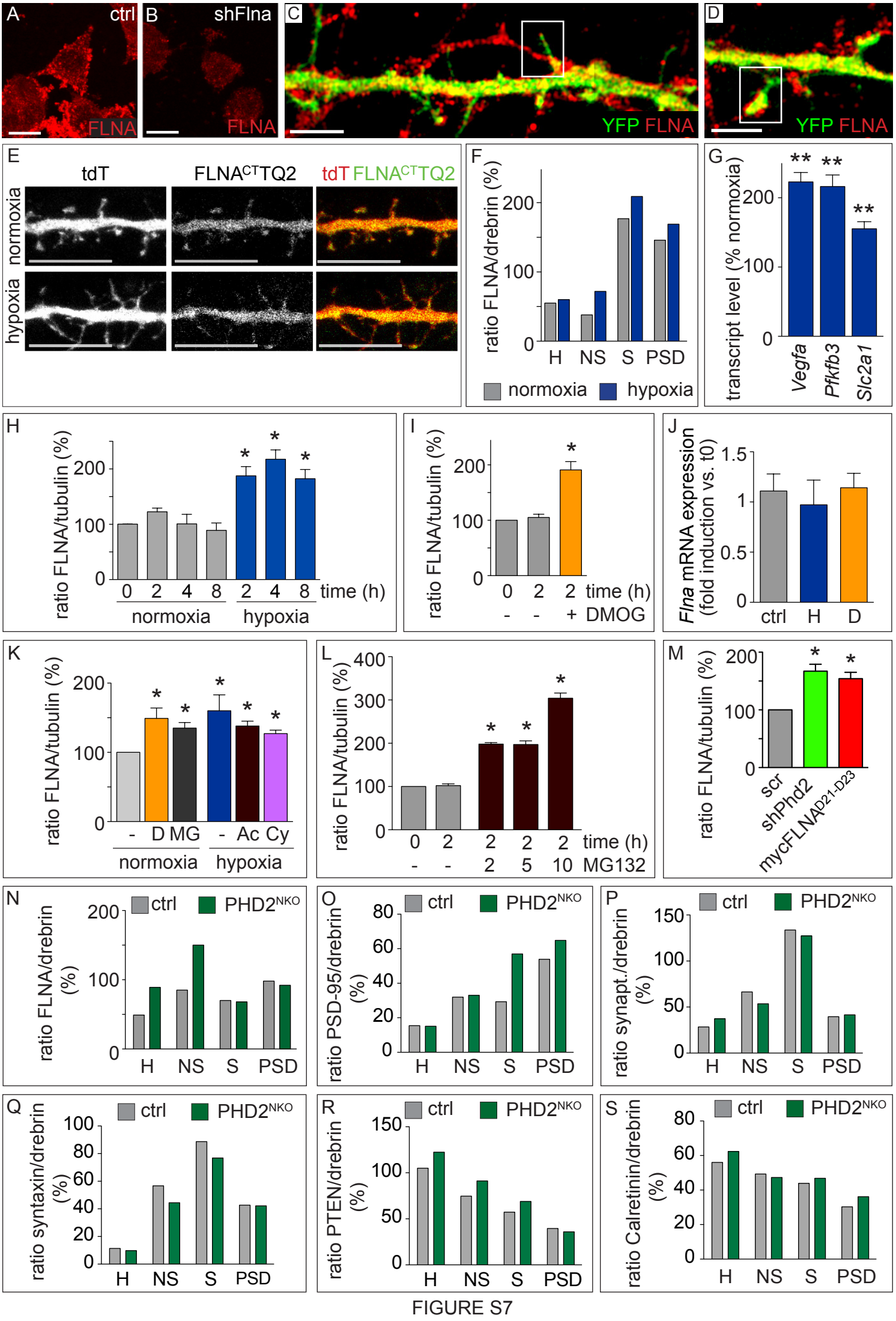
A
ctrl
FLNA
B
shFlna
FLNA
C
YFP FLNA
D
YFP FLNA
E
tdT
FLNA^CTTQ2
tdT FLNA^CTTQ2
normoxia
hypoxia
F
ratio FLNA/drebrin (%)
200
100
0
H NS S PSD
normoxia
hypoxia
G
transcript level (% normoxia)
200
100
0
**
**
**
Vegfa
Pfkfb3
Slc2a1
H
ratio FLNA/tubulin (%)
200
100
0
* * *
0 2 4 8 2 4 8 time (h)
normoxia
hypoxia
I
ratio FLNA/tubulin (%)
200
100
0
*
0 2 2 time (h)
- - + DMOG
J
Flna mRNA expression
(fold induction vs. t0)
1.5
1
0.5
0
ctrl H D
K
ratio FLNA/tubulin (%)
200
100
0
* * * * *
- D MG - Ac Cy
normoxia
hypoxia
L
ratio FLNA/tubulin (%)
400
300
200
100
0
* * *
0 2 2 2 2 time (h)
- - 2 5 10 MG132
M
ratio FLNA/tubulin (%)
200
100
0
* *
scr
shPhd2
mycFLNA^D21-D23
N
ratio FLNA/drebrin (%)
ctrl
PHD2^NKO
200
100
0
H NS S PSD
O
ratio PSD-95/drebrin (%)
ctrl
PHD2^NKO
80
60
40
20
0
H NS S PSD
P
ratio synapt./drebrin (%)
ctrl
PHD2^NKO
150
100
50
0
H NS S PSD
Q
ratio syntaxin/drebrin (%)
ctrl
PHD2^NKO
100
80
60
40
20
0
H NS S PSD
R
ratio PTEN/drebrin (%)
ctrl
PHD2^NKO
150
100
50
0
H NS S PSD
S
ratio Calretinin/drebrin (%)
ctrl
PHD2^NKO
80
60
40
20
0
H NS S PSD

FIGURE S7

FIGURE S7; RELATED TO FIGURE 4

A,B, PC12 cells in control conditions (ctrl, A) or after silencing of *Flna* (shFlna, B), and immunostained for FLNA (red). **C,D,** Representative images of YFP transfected RHNs immunostained for endogenous FLNA (red). Boxes denote regions that are shown at higher magnification in Fig. 4A. **E,** 14 DIV MHNs co-transfected with tdT (red) and C-terminus FLNA-TQ2 ($FLNA^{CT}TQ2$, green) incubated in normoxia (top) or hypoxia (bottom) for 16 hr. Left and middle panels: single tdT or $FLNA^{CT}TQ2$ signal channel, respectively, in gray scale. The right panels: merged images. **F,** Densitometric quantifications of the ratio of FLNA protein levels (normalized to drebrin) of the immunoblot (IB) shown in Fig. 4C. **G,** Quantification of mRNA transcripts of HIF-target genes. Two weeks old mice were maintained under normal atmospheric conditions or exposed to hypoxia (8% O_2) for 4-5 hr before sacrifice. mRNA was isolated from the brains and quantified by RNA-Seq (n = 3 mice). *Vegfa*, vascular endothelial growth factor A; *Pfkfb3*, phosphofructokinase-2/fructose-2,6-bisphosphatase 3; *Slc2a1*, solute carrier family 2 (facilitated glucose transporter) member 1 (Glut1). **H**, Densitometric quantification of FLNA IBs from 14 DIV MHNs incubated under hypoxia for the indicated time points (expressed in % of the value at 0 hr in normoxia, n = 5). A representative blot is shown in Fig. 4D. **I**, Densitometric quantification of FLNA IBs from 14 DIV MHNs treated for 2 hr without or with DMOG (n = 4). A representative blot is shown in Fig. 4E. **J,** Quantification of *Flna* transcript levels in MHNs under control (ctrl), hypoxia (H) or DMOG (D) treatment for 4 hr, normalized to the value at 0 hr (n = 3). **K**, Densitometric quantification of FLNA IBs from homogenates of MHNs in normoxia or hypoxia in the absence (-) or presence of DMOG (D), MG132 (MG), actinomycin D (Ac) or cycloheximide (Cy) (expressed in % of the value in untreated MHNs in normoxia, n = 3). A representative blot is shown in Fig. 4F. **L**, Densitometric quantification of FLNA IBs from homogenates of MHNs treated for 2 hr with increasing concentrations of MG132 (expressed in % of the value in untreated MHNs at 0 hr, n = 3). A representative blot is shown in Fig. 4G. **M**, Densitometric quantifications of FLNA IBs from homogenates of MHNs transduced with scr, shPhd2 or overexpressing myc-tagged FLNA deletion mutant D21-D23 ($mycFLNA^{D21\text{-}D23}$) (n = 3). A representative blot is shown in Fig. 4H. **N-S,** Densitometric quantifications of the levels of FLNA (N), the postsynaptic marker PSD-95 (O), the presynaptic markers synaptophysin (P) and syntaxin (Q) and of soluble fraction enriched markers PTEN (R) and calretinin (S) in mouse brain homogenate (H), non-synaptic fraction (NS), synaptic membranes (S) and PSD subfractions obtained from control (ctrl) or $PHD2^{NKO}$ littermates, as shown in the IBs in Fig. 4I. Data are mean ± SEM. *$p < 0.05$, **$p < 0.01$. Scale bar, 10 μm (A,B,E), 2 μm (C,D).

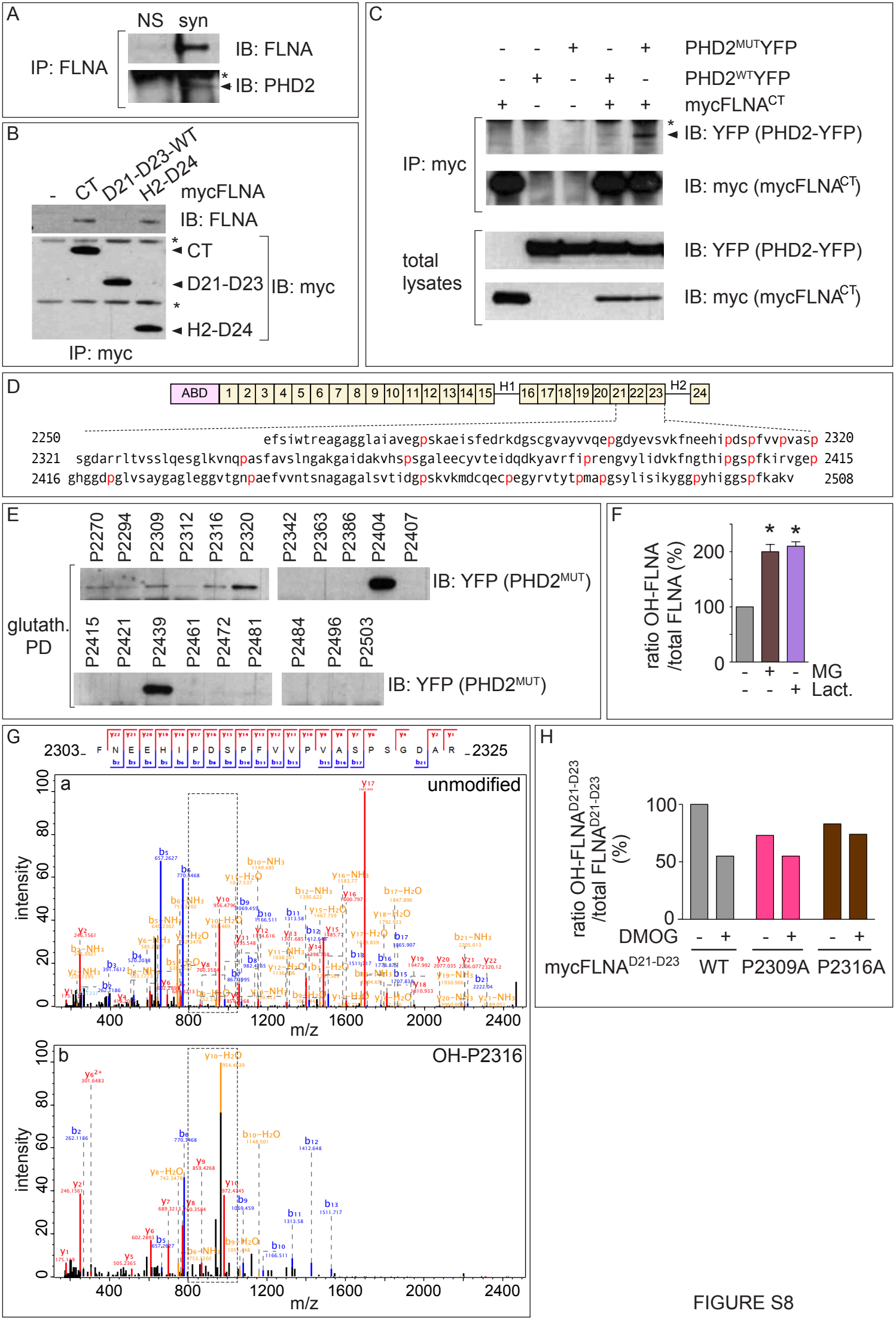
A
NS syn
IP: FLNA
IB: FLNA
IB: PHD2
B
- CT D21-D23-WT H2-D24 mycFLNA
IB: FLNA
CT
D21-D23
H2-D24
IB: myc
IP: myc
C
PHD2MUTYFP
PHD2WTYFP
mycFLNACT
IB: YFP (PHD2-YFP)
IP: myc
IB: myc (mycFLNACT)
total lysates
IB: YFP (PHD2-YFP)
IB: myc (mycFLNACT)
D
ABD 1 2 3 4 5 6 7 8 9 10 11 12 13 14 15 H1 16 17 18 19 20 21 22 23 H2 24
2250 efsiwtreagagglaiavegpskaeisfedrkdgscgvayvvqepgdyevsvkfneehipdspfvvpvasp 2320
2321 sgdarrltvsslqesglkvnqpasfavslngakgaidakvhspsgaleecyvteidqdkyavrfiprengvylidvkfngthipgspfkirvgep 2415
2416 ghggdpglvsaygagleggvtgnpaefvvntsnagagalsvtidgpskvkmdcqecpegyrvtytpmapgsylisikyggpyhiggspfkakv 2508
E
P2270 P2294 P2309 P2312 P2316 P2320 P2342 P2363 P2386 P2404 P2407
IB: YFP (PHD2MUT)
glutath. PD
P2415 P2421 P2439 P2461 P2472 P2481 P2484 P2496 P2503
IB: YFP (PHD2MUT)
F
ratio OH-FLNA /total FLNA (%)
200
100
0
MG
Lact.
G
2303- F N E E H I P D S P F V V P V A S P S G D A R -2325
a
unmodified
intensity
m/z
b
OH-P2316
H
ratio OH-FLNAD21-D23 /total FLNAD21-D23 (%)
100
50
0
DMOG
mycFLNAD21-D23
WT P2309A P2316A

FIGURE S8

FIGURE S8; RELATED TO FIGURE 5

A, Representative IB for FLNA and PHD2 after immunoprecipitation (IP) of FLNA from non-synaptic (NS) and synaptic membrane (syn) subfractions of the brain of 2 weeks old mice. Arrow indicates PHD2, asterisk indicates the heavy chain of the IgGs used for the IP. **B,** Representative IB for myc and FLNA after IP of myc from HEK293T cells expressing myc-tagged FLNA deletion mutants mycFLNA^{CT} (CT), mycFLNA$^{D21\text{-}D23\text{-}WT}$ (D21-D23) or mycFLNA$^{H2\text{-}D24}$ (H2-D24). Arrows indicate the myc-tagged deletion mutants; asterisks indicate the heavy and light chains of the IgGs used for the IP. **C,** Representative IB for myc and YFP after IP of myc from HEK293T cells expressing mycFLNA^{CT}, PHD2^{WT}YFP or PHD2^{MUT}YFP alone or a combination of them. Arrow indicates the PHD2 after the IP; asterisk indicates aspecific band. Total lysate controls are shown (bottom). **D,** Amino acid sequence of the D21-D23 deletion mutant of FLNA that interacts with PHD2. Each line corresponds to the sequence of the different domains. The proline residues are indicated in red. **E,** Recombinant GST-fusion peptides, each containing a proline residue in FLNA$^{D21\text{-}D23\text{-}WT}$ (flanked by 6 amino acids upstream and downstream of the respective proline residue), were incubated with homogenates of HEK293T cells expressing PHD2^{MUT}YFP. Glutathione-beads were used to pull-down the complexes, and bound PHD2^{MUT}YFP was identified by IB for YFP. **F,** Densitometric quantification of hydroxyl-FLNA level in HEK293T cells transfected with myc-FLNA and treated for 2 hr with MG132 (MG) or lactacystin (Lact.) (n = 3). A representative IB is shown in Fig. 5E. **G**, MS/MS fragmentation spectra of the unmodified (a) and hydroxylated P2316 (b; OH-P2316) sequence FNEEHIPDSPFVVPVASPSGDAR of FLNA. The boxed areas comprising the peaks corresponding to the proline P2316 containing fragments y10 are shown at larger scale in Fig. 5G. **H,** Densitometric quantification of the ratio hydroxylated/total mycFLNA$^{D21\text{-}D23}$ protein levels of IB from homogenates of HEK293T cells co-transfected with PHD2^{WT}YFP together with mycFLNA$^{D21\text{-}D23\text{-}WT}$, mycFLNA$^{D21\text{-}D23\text{-}P2309A}$ or mycFLNA$^{D21\text{-}D23\text{-}P2316A}$ in the absence or the presence of DMOG. The corresponding blot is shown in Fig. 5H. Data are mean ± SEM. *$p < 0.05$.

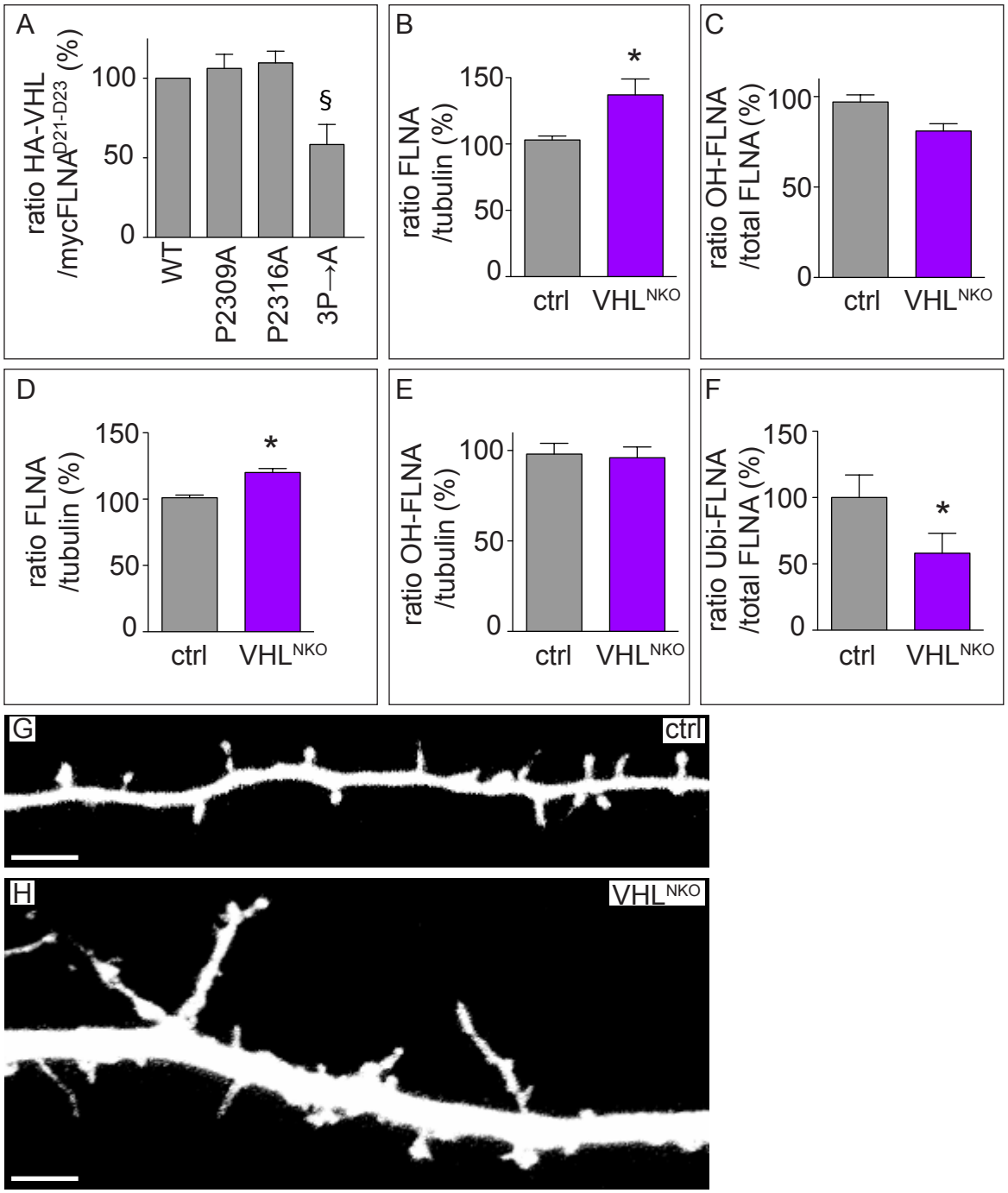
A
ratio HA-VHL /mycFLNA$^{D21-D23}$ (%)
100
50
0
§
WT
P2309A
P2316A
3P→A
B
ratio FLNA /tubulin (%)
150
100
50
0
*
ctrl
VHL^{NKO}
C
ratio OH-FLNA /total FLNA (%)
100
50
0
ctrl
VHL^{NKO}
D
ratio FLNA /tubulin (%)
150
100
50
0
*
ctrl
VHL^{NKO}
E
ratio OH-FLNA /tubulin (%)
100
50
0
ctrl
VHL^{NKO}
F
ratio Ubi-FLNA /total FLNA (%)
150
100
50
0
*
ctrl
VHL^{NKO}
G
ctrl
H
VHL^{NKO}

FIGURE S9

FIGURE S9; RELATED TO FIGURE 6

A, Densitometric quantification of the ratio of interaction between HA-VHL with wild type (WT) or mutant mycFLNA$^{D21-D23}$ (P2309A, P2316A or P2309/2312/2316A (3P→A)) (n = 3). A representative immunoblot (IB) is shown in Fig. 6C. **B**, Densitometric quantification of FLNA levels in brain homogenates obtained from E14.5 control (ctrl) or VHL^{NKO} littermates (n = 3-4 mice). The corresponding IB is shown in Fig. 6E. **C-E,** Densitometric quantification of the ratio of hydroxylated FLNA over total FLNA (C), FLNA protein level (D) or total hydroxyl-FLNA level (normalized to tubulin) (E) in brain homogenates obtained from E14.5 control (ctrl) or VHL^{NKO} littermates (n = 3-4 mice). The corresponding IB is shown in Fig. 6F. **F,** Densitometric quantification of the ubiquitinated-FLNA/total FLNA ratio in brain homogenates obtained from E14.5 control (ctrl) or VHL^{NKO} littermates and subjected to TUBE2 pull-down. The corresponding IB is shown in Fig. 6G (n = 2 mice). **G,H,** Representative images of 14 DIV MHNs from control (ctrl, G) or VHL^{NKO} (H) littermates and transfected with tdT. Data are mean ± SEM. * $p < 0.05$; § $p = 0.07$. Scale bar, 10 μm (G,H).

SUPPLEMENTAL EXPERIMENTAL PROCEDURES

ANIMALS

Animal housing and experimental procedures were approved by the Animal Ethics Committee of the KU Leuven (Belgium). *Wild type* (WT) Swiss mice and Wistar rats were used. *Phd2*$^{lox/lox}$ (Mazzone et al., 2009), PHD2-KO (Mazzone et al., 2009) and *Nestin*Cre (Tronche et al., 1999) mice had C57BL6 background. *Vhl*$^{lox/lox}$ (Haase et al., 2001) and *Hif-1α*$^{lox/lox}$ (Ryan et al., 2000) mice had BALB/c-C57BL6 mixed background.

MHN ISOLATION, CELL CULTURE, TRANSFECTION AND TRANSDUCTION

MOUSE AND RAT HIPPOCAMPAL NEURONS were isolated as previously described (Segura et al., 2007), and plated on coverslips or tissue culture plates coated with 0.2 mg/ml poly-D-lysine (Sigma) and 5 µg/ml laminin (Life Technologies). For the washout experiments, neurons were plated on culture plates marked with a grid (500 µm grid distance; IBIDI). Neurons were cultured in neurobasal medium supplemented with 1X B27 and 0.5 mM glutamine (all from Life Technologies). The neuronal density was 50-70,000 neurons per 24-well plate or 500,000 neurons per p35-dish (equivalent to 325-450 cells/mm^2). For in vitro electrophysiological experiments, cells were seeded on conventional glass coverslips or on substrate-integrated multi-electrode arrays at a density of 1,000 cells/mm^2 or 3,200 cells/mm^2, respectively. Neurons were grown for 7-14 days in vitro (DIV) and transfected with Lipofectamine2000 (Life Technologies) following the manufacturer's instructions, and analyzed at 14 or 21 DIV. When indicated, 3-5 DIV neurons were transduced overnight (o/n) using 10 MOI lentiviral particles. For adenoviral particles, isolated MHN were incubated with 10 MOI particles for 15 min before plating. *HUMAN EMBRYONIC KIDNEY (HEK) 293T CELLS* were maintained in Dulbecco Modified Earl Media (DMEM) supplemented with 10% fetal bovine serum (FBS), 2 mM glutamine, 100 U/ml penicillin and 10 µg/ml streptomycin (all from Life Technologies). HEK293T cells were transfected by the calcium phosphate precipitation method. When indicated, cells were treated with the following concentrations of compounds: 250 µM DMOG (Enzo Life Sciences), 10 µM MG132 (Calbiochem), 10 µM lactacystin (Millipore), 5 µM acriflavine (Sigma), 1 µg/ml actinomycin D (Sigma), 20 µg/ml cycloheximide (Sigma). *RAT PC12 CELLS* were maintained in DMEM supplemented with 5% FBS, 5% horse serum, 2 mM glutamine, 100 U/ml penicillin and 10 µg/ml streptomycin (all from Life Technologies). PC12 cells were transfected with siRNA sequences for either rat PHD2 or FLNA (IDT Trifect) by nucleofection, program U29 (AMAXA). Cells were routinely maintained in culture at 37ºC, 5% CO_2 and 21% O_2. Hypoxic incubations were made in a 94% N_2, 5% CO_2, 1% O_2 atmosphere for neurons, and 94.8% N_2, 5% CO_2, 0.2% O_2 for HEK293T cells.

MORPHOGENESIS OF DENDRITIC SPINES IN NORMOXIA

To characterize dendritic spines in vitro, we first monitored the maturation of dendritic spines in monocultures of mouse hippocampal neurons (MHNs) during 21 days in vitro (DIV). To visualize single dendritic protrusions, we transfected 6 DIV MHNs with yellow fluorescent protein (YFP), enhanced green fluorescent protein (EGFP) or tandem dimer tomato (tdT) fluorescent protein. At 8 DIV, MHNs extend few, long immature dendritic protrusions (Fig. S1A-C). Three days later, more numerous dendritic protrusions extended from dendrites (Fig. S1A) and progressively matured over time towards shorter mushroom-shaped spines at 15 DIV (Fig. S1A-C). Beyond 16 DIV, dendritic spine density and maturation were maintained (not shown).

To determine whether the morphological analysis of dendritic spine maturation correlated with neuronal activity, we used multi-electrode arrays (MEAs) to record the spontaneous action potentials (APs) fired by the neuronal network. These electrophysiological experiments revealed that the morphological maturation of the dendritic spines was accompanied by

increased synaptic activity. Indeed, over time and concomitant with morphological spine maturation, cultured MHNs acquired a spontaneous synchronized network-wide spiking activity that was evident after 12 DIV (Fig. S1A-E), as previously reported for ex vivo developing networks (Marom and Shahaf, 2002). Taken together, our morphological analysis and electrophysiology recordings, together with previous reports (Nwabuisi-Heath et al., 2012; Ziv and Smith, 1996), showed that dendritic spines of 14 DIV MHNs were undergoing progressive maturation.

SYNAPTOSOMAL FRACTIONATION

Post-synaptic density fractionations were prepared from brains obtained from 2 weeks old animals (mice or rats), as previously described (Cho et al., 1992), with inclusion of 10 μM of the proteasomal inhibitor MG132 in the lysis buffer.

PLASMIDS AND LENTIVIRAL VECTORS

The following plasmids were previously reported: pEYFP-N1 (Clontech), pcDNA3-myc-hFLNA-WT (Addgene #8982; transcript 1, UniProtID: Q60FE5 (Woo et al., 2004)), p-sh-SCR and p-shPHD2 (Leite de Oliveira et al., 2012; Mazzone et al., 2009), pRSET-B-tdTomato (Shaner et al., 2004), 9xHRE::Luciferase (Aragones et al., 2001), pBrainbow1.0 (Livet et al., 2007), pOG231-NLS-Cre (O'Gorman et al., 1991), HA-VHL-pRc/CMV (Addgene #19999 (Iliopoulos et al., 1995)), pCAGGS-GFP (Niwa et al., 1991) and pCAGGS-RFP-11 (Attardo et al., 2008). Murine *Phd2* was cloned in frame in the pEYFP-N1 vector, to generate the $PHD2^{WT}$YFP fusion protein. The myc-tagged deletion mutants of hFLNA were generated by PCR from the pcDNA3-myc-hFLNA-WT plasmid. The TQ2-labeled full-length and C-terminus (2250-2639 aa.) of *hFLNA* were cloned in frame in the pTQ2-N1 plasmid (Goedhart et al., 2012). The $PHD2^{MUT}$YFP mutants (H290A/D292A (Vogel et al., 2010), mycFLNA$^{D21\text{-}D23\text{-}P2309A}$, mycFLNA$^{D21\text{-}D23\text{-}P2316A}$ and mycFLNA$^{D21\text{-}D23\text{-}3P\rightarrow A}$ (P2309/2312/2316A) were generated using the QuickChange mutagenesis kit (Stratagene). GST-fusion proteins were made by cloning the coding sequence of the *FLNA* fragments in the pGEX4-T2 plasmid (GE Healthcare). Lentiviral vectors were made using the pLVx-shRNA2 (scr, shPhd2, shPhd1, shFlna; Clontech), pLKO (scr, shVhl; Sigma) or pRRL (mycFLNA(D21-D23)) backbones.

LUCIFERASE ACTIVITY

Cells expressing Firefly luciferase were lysed and enzymatic luciferase activity was measured in a Microlumat LB96V Luminometer (Berthold Technologies).

IMMUNOBLOTS, IMMUNOPRECIPITATIONS AND PULL-DOWNS

For immunoblots, protein samples were separated by SDS-PAGE and transferred to 0.45-mm nitrocellulose membranes (Life Technologies). For immunoprecipitation, cells or tissue from mice or rats were lysed in chilled lysis buffer (50 mM Tris-HCl pH 7.5, 150 mM NaCl, 0.1% Triton-X100, 0.1% Brij35, 10% glycerol, 10 μM MG132 1% Complete protease inhibitor and 1% PhosSTOP (both from Roche)), and centrifuged at 15,000g for 10 min at 4ºC. Antibodies were pre-bound to protein A– or protein G–coated Dynabeads (Life Technologies) or agarose beads (Pierce or GE Healthcare). Lysates were incubated for 2 hr-o/n at 4ºC. To isolate ubiquitinated proteins, samples were lysed in cold lysis buffer containing 10 μM PR-619 (Sigma), and centrifuged at 15,000g for 10 min at 4ºC. Lysates were incubated with agarose-TUBE2 (Life Sensors) for 16 hr. In vitro binding assays were performed with GST-fusion proteins (expressed in *E. coli* BL21-Gold (DE3; Life Technologies)) and cell homogenates obtained from HEK293T cells transfected with YFP or $PHD2^{MUT}$YFP, and incubated for 2 h at 4ºC. GST complexes were pulled-down with glutathione-coated beads (GE Healthcare). For antibodies used in immunoblots, see below.

RNA ANALYSIS

IN SITU HYBRIDIZATION: In situ hybridizations (ISH) were made as previously reported (Ruiz de Almodovar et al., 2011), using DIG-labeled antisense probes for murine *Phd1 (Egln2)*, *Phd2 (Egln1)* or *Phd3 (Egln3)* or sense probes as control on PFA fixed cryosections or free-floating vibratome sections. *RT-PCR:* Cells were lysed and total RNA was isolated using the PureLink RNA Mini Kit (Life Technologies). Complementary DNA was synthetized by the QuantiTect Retrotranscriptase reaction (Qiagen). RNA expression analysis was performed by Taqman quantitative RT-PCR using in house-designed primers and probes or premade primer sets (IDT). Sequences or ID numbers are available upon request. *RNA-SEQ*: Brains of 2 weeks old mice were collected and total RNA was isolated using TRIZOL (Life technologies). Quantitative RNA-seq analysis (Illumina) was performed by the Genomics Core (KU Leuven-UZ Leuven).

IMMUNOHISTOCHEMISTRY

Immunohistochemical stainings were performed on 4% PFA fixed MHN or thick free-floating brain cryosections. Samples were permeabilized with PBS-0.1% Triton X-100, and blocked with 10% goat serum. Primary antibodies (see below) were incubated o/n at 4ºC. Secondary antibodies were Alexa-488, -568 -633 or -647 conjugated antibodies (Life Technologies). Slides were mounted with ProLong-Gold anti-fade mounting media containing DAPI (Life Technologies). Analysis of spines in vivo was made in 80-100 µm vibratome sections. Golgi staining was performed in 2 weeks old littermates, using the FD Rapid Golgi Stain Kit (FD NeuroTechnologies). TUNEL staining was performed in 4% PFA fixed MHN using the *In Situ* Cell Death Detection Kit (Roche).

ANTIBODIES

The following antibodies were used: rabbit anti-PHD2 (Novus); mouse anti-myc (9E10) and rabbit anti-FLNA (for IHC of rat FLNA) (Santa Cruz); rabbit anti-FLNA (for mouse FLNA in IB), rabbit anti-hydroxyprolines, rabbit anti-PSD-95 and rabbit anti-drebrin (Abcam); mouse anti-FLNA (for IP of rat FLNA), mouse anti-PSD-95 and guinea pig anti-vGlut1 (Millipore); mouse anti-GFP (JL8, Clontech); rabbit anti-GFP (Fitzgerald); mouse anti-α-tubulin and rabbit anti-syntaxin (Sigma); rabbit anti-β-actin, rabbit anti-cleaved caspase 3, rabbit anti-pVHL and rabbit anti-PTEN (Cell Signaling); mouse anti-synaptophysin and rabbit anti-ubiquitin (Dako); rat anti-HA (Roche); goat anti-HIF-1α (R&D Systems); rabbit anti-PARP1 (Enzo); rabbit anti-calretinin (Swant Inc.).

MASS SPECTROMETRY

IN GEL PROTEIN DIGESTION: Stained protein bands were excised from the gel, and in-gel tryptic digestion was performed as described previously (Wilm et al., 1996) with minor modifications. Briefly, after several washing steps (50 mM NH_4HCO_3 / 50% acetonitrile (ACN)) to eliminate the stain, the protein were reduced (10 mM DTT in 50 mM NH_4HCO_3 for 30 min at 56°C) and then alkylated (55 mM iodoacetamide in 50 mM NH_4HCO_3 for 30 min at room temperature in the dark). The gel pieces were washed in 50 mM NH_4HCO_3 and then dried in 100% ACN to be rehydrated in a sufficient covering volume of Trypsin solution (10 ng/µl in 10 mM NH_4HCO_3; Promega). Trypsin digestions were performed o/n at 37°C with shaking. Peptides were extracted once with 50 mM NH_4HCO_3, twice 5 % formic acid (FA) in 50% ACN and once with 100% ACN. The five extractions were combined and the mixture was dried down in a vacuum concentrator and then reconstituted in 12 µl H_2O/ACN/FA (98:2:0.1). *MASS SPECTROMETRY ANALYSIS, DATABASE SEARCH, AND PROTEIN IDENTIFICATION:* Digested peptides were analyzed by nano LC-MS/MS using an EASY-nLC 1000 (Thermo Fisher Scientific) coupled to a Q Exactive Orbitrap mass spectrometer. 5 µl of each sample were picked up at 300 nl/min, loaded on a home-made C_{18} 18 cm capillary column picotip silica emitter tip (75 µm diameter filled with 1.9 µm Reprosil-Pur Basic C_{18}-HD resin (Dr. Maisch GmbH, Ammerbuch-Entringen, Germany)) equilibrated in solvent A (0.1 % FA). The peptides were eluted using a 2 to 50 % two

slopes gradient of solvent B (0.1 % FA in ACN) during 47 min at 250 nl/min flow rate (total length of the chromatographic run was 80 min). The Q Exactive (Thermo Fisher Scientific) was operated in data-dependent acquisition mode with the XCalibur software (Thermo Fisher Scientific). Survey scan MS were acquired in the Orbitrap on the 300 – 1800 *m/z* range with the resolution set to a value of 70,000 at *m/z* = 400 in profile mode (AGC target at 1^E6). The 15 most intense ions per survey scan were selected for HCD fragmentation (NCE 28), and the resulting fragments were analyzed in the Orbitrap at 35,000 of resolution (m/z 400). Isolation of parent ion was set at 2.5 m/z and Underfill ratio at 2.5%. Dynamic exclusion was employed within 30 s. Data were searched using MaxQuant (1.4.1.2 version) (with the Andromeda search engine) against the human database from SwissProt and TrEMBL (Jan 21st 2014, 88,500 entries, of which 39,715 from SwissProt). The following search parameters were applied: Carbamidomethylation of cysteines was set as a fixed modification, and oxidation of methionine, protein N-terminal acetylation and Oxidation of Proline were set as variable modifications. The mass tolerances in MS and MS/MS were set to 10 ppm for each, respectively. Maximum peptide charge was set to 7 and 5 amino acids were required as minimum peptide length. Peptides and proteins identified with an FDR lower than 0.1% were considered as valid identification. For *GSSG/GSH MEASUREMENT*, lysates from 14 DIV control or treated MHNs were collected and the level of GSSG in percent of GSSG + GSH was determined using liquid chromatography-mass spectrometry. As positive control, MHN were treated with 100 μM H_2O_2 for 1 hr.

IN-UTERO ELECTROPORATION

Pregnant mice were isofluorane anaesthetized at E15.5 and laparotomy was performed to expose the uteri. Circa 2 μl of PBS containing 5 mg/ml of plasmid was injected into the lumen of the embryonic forebrain followed by electroporation of the hippocampal anlage using 8 pulses of 40 V, 50 ms each at 1 s interval delivered through platinum electrodes using a BTX-830 electroporator (Genetronics) as previously described (Pacary et al., 2012). Dendritic morphology of hippocampal CA1 neurons was investigated at P15. Briefly, mice were intracardially perfused with 4% PFA, and brains were removed and post-fixed for additional 24 h in 4% PFA. Brains were dissected and post-fixed in the same solution overnight at 4°C. Coronal brain sections (100 μm thick) were cut on a vibratome and mounted with Prolong antifade mounting media (Life Technologies) and imaged.

IMAGING AND TIME-LAPSE RECORDINGS

IMAGING was performed using a Zeiss LSM 510 Meta NLO, Zeiss LSM 780 confocal microscope (oil immersion objectives EC Plan-Neofluar 40x with NA 1.3, Plan-Apochromat 63x with NA 1.4, and alpha Plan-Apochromat 100x with NA 1.46) (Carl Zeiss) or Leica SP8x confocal microscope (Leica) (oil immersion objective 63x with NA 1.4). Bright field images were acquired with an Axioplan-2 microscope coupled to an Axiocam HRc (Carl Zeiss). For *TIME-LAPSE IMAGING UNDER NORMOXIA*, pictures were acquired every 5 min for 4 h at 37°C using a Zeiss LSM 780 confocal microscope. In the case of DMOG treatment, the movie started just when the drug was added on the culture media. For *TIME-LAPSE UNDER HYPOXIA*, cells were under 0.5% O_2, 5% CO_2 and 37ºC (GM230 Tri-Gas Mixer, CellASIC ® Onix Microfluidic Platform, Millipore) and images were captured every 5 min for 4 h at 37°C using a Zeiss LSM 510 Meta NLO. The movie just started when switching the cultures to hypoxic conditions. *SUPER-RESOLUTION IMAGING* was performed using a Zeiss Elyra Structured Illumination microscope (SR-SIM) (Carl Zeiss) equipped with an oil 63x Plan-Apochromat objective with NA 1.4, three SIM grid rotations and averaging 4 scans of each pixel. *FLIM-FRET:* Time-domain fluorescence lifetime imaging microscopy (FLIM) was performed in transiently transfected HEK293T cells grown on glass-bottom dishes and transfected with the indicated plasmids. FLIM data were obtained using a confocal laser-scanning Leica TCS SP5 microscope. A pulsed two-photon Titanium:sapphire laser (Mai Tai HP, Spectra Physics, Newport) tuned at 820 nm was used for excitation. The excitation light was directed to the sample through a 63x (NA 1.2) water immersion objective. The emission light was filtered using a short pass 665 nm filter and a BP480/40 nm band pass filter. Finally, an APD detector (H7429-40,

Hamamatsu) connected to PicoQuant TCSPC hardware (PicoQuant) was used to detect the emission light, allowing for time-correlated single photon counting. FLIM images were processed using SymPhoTime software (PicoQuant). The quality of the fit was judged by the reduced χ^2–values. For the majority of the pixels the reduced χ^2–value was smaller than 1.2. *GOLGI IMPREGNATION:* To detect the Golgi impregnation, the Zeiss LSM780 confocal microscope was automatically set up in reflection mode by using a 488 nm wavelength and replacing the dichroic filter by a 20/80 beam splitter (Spiga et al., 2011). Images were acquired with an alpha Plan-Apochromat 100x/1.46 oil objective. No barrier filter was used to direct the reflected light by the sample to the detector. *ELECTRON MICROSCOPY* was performed using a JEM-1400 transmission electron microscope (Jeol, Zaventem, Belgium), equipped with an 11Mpixel Olympus SIS Quemesa camera. Ctrl and $PHD2^{NKO}$ littermates were processed as previously described (Arranz et al., 2015). Briefly, mice (n=3-4 mice) were transcardially perfused with 2.5% glutaraldehyde, 2% paraformaldehyde in 0.1 M cacodylate buffer. Brains were dissected and post-fixed in the same solution overnight at 4°C. Coronal brain sections (300 µm thick) were cut on a vibratome and rectangular pieces of tissue comprising the *striatum* were dissected. Tissue was post-fixed with 1% OsO_4, 1.5% $K_4Fe(CN)_6$ in 0.1 M cacodylate buffer, rinsed, stained with 3% uranyl acetate and dehydrated in graded ethanols and propyleneoxide, followed by embedding in EMbed812. Ultrathin sections (70nm) were obtained using an ultramicrotome (Leica Reichert Jung Ultracut E), mounted on 400 mesh copper grids and contrasted with uranyl acetate and lead citrate before being imaged. Images were taken at 2500X magnification.

MORPHOMETRIC ANALYSIS AND QUANTIFICATIONS

MORPHOMETRIC ANALYSIS AND QUANTIFICATIONS were done in primary and secondary dendrites, and the protrusions included in these dendrites. Synaptic density was assessed as previously described (Segura et al., 2007). Quantifications were done with NIH ImageJ software, using neurons from 3 independent experiments (isolations), with $n \geq 7$ neurons per condition/experiment, unless otherwise stated. All quantifications and manual counting were performed by persons, blinded for the experimental conditions. *QUANTIFICATION OF PROTRUSION LENGTH IN TIME-LAPSE MOVIES* was determined as follows. We measured the length of the spines, at the starting point and after different time points. Spines with variations ≤0.2 µm were considered stable. All imaged spines were measured at the starting point (0 hr) and end (1 hr for hypoxia or 4 hr for DMOG and shPhd2) of the time-lapse imaging (Fig. 1G,O; Fig. 3O). For the quantifications monitored over time at different time intervals using control or DMOG-treated neurons (Fig. S2A), we selected spines that were ≤2 µm long at the start of the analysis (≈75-80% of the spines were ≤2 µm in both cases), since this is the length of mature spines in the hippocampus (Sorra and Harris, 2000). We then followed over time how these spines responded to control vehicle or DMOG treatment. To evaluate the effect of PHD2 silencing, MHNs were transfected at 7 DIV with scr or shPhd2 constructs, and evaluated at 7 days later. Spines showed differences in length (spines >2 µm: ≈25% for scr vs. ≈70% for shPHD2), and they were randomly selected for quantification (Fig. S3K). *SYNAPTIC DENSITY IN VIVO* was determined by transmission electron microscopy or by measuring the $PSD\text{-}95^+$ or $synaptophysin^+$ fluorescent signal detected per area unit of the stratum radiatum of the CA1 hippocampal region. For the latter analysis, the same threshold was set for all the images. *QUANTIFICATION OF SYNAPTIC DENSITY IN VITRO* was determined as previously reported (Hotulainen et al., 2009; Kayser et al., 2008; Segura et al., 2007). Briefly, to identify single dendrites, we transfected MHN at 14 DIV either with YFP (green) or tdTomato (tdT; red) fluorescent proteins, and performed the staining at 21 DIV. We performed two different stainings: (I) anti-vGlut and anti-PSD-95 co-staining or (II) anti-synaptophysin staining. In the first case, we counted the number of $vGlut^+/PSD\text{-}95^+$ co-clusters that were localized on the fluorescently labeled dendrite. In the second case, for every single dendrite analyzed, we counted only those synaptophysin-positive clusters, (i) in which immunoreactive signal completely colocalized with the positive signal of the dendrite to yield a yellow cluster, or (ii) in which the immunoreactive signal was in immediate close apposition with ("touching") the positive signal of a dendrite or its spines, when analyzed with a 63-fold magnification. Under those conditions, the distance between the "touching" (red or green) signals was <200nm. *GENERAL NOTE:* In all panels showing immunostaining of neuronal cultures for vGlut1, synaptophysin, PSD95,

PHD2 or FLNA, immunoreactive signals are not only confined to the contours of the neuron under investigation (transfected with a fluorescent reporter to reveal its dendritic protrusions), but are also detectable as positive stainings in neighbouring neurons, which themselves are however not transfected with a fluorescent reporter and therefore their cell body is not visible in the image. High-density cultures had to be used to allow maintenance of the neuronal cultures for prolonged periods; transfection with fluorescent reporters (see above) was done using conditions transfecting only a fraction of the neurons to allow visualization of single neurons.

CELLULAR AND NETWORK ELECTROPHYSIOLOGY

Patch-clamp recordings of the membrane electrical potential of cultured hippocampal neurons were performed at 14 and 21 days after plating, as described (Reinartz et al., 2014) from the cell somata, under the whole-cell configuration using an Axon Multiclamp 700B Amplifier (Molecular Devices LLC, Sunnyvale, CA, USA), in current-clamp mode. Overnight hypoxic treatment or incubations with DMOG (250 μM) were performed the day prior the recordings. Patch electrodes were pulled from standard borosilicate glass (1B150F-4, World Precision Instruments, Sarasota, FL, USA) by a horizontal puller (P97, Sutter, Novato, CA, USA) to a resistance of 6-7MΩ. Electrodes were filled with an intracellular solution containing (in mM): 135 K-gluconate, 10 KCl, 10 HEPES, 0.2 EGTA, 4 Mg-ATP, 0.4 Na_3GTP, and 14 Na_2-phosphocreatine (pH 7.3, titrated with KOH). All recordings were obtained at 34°C shortly after replacing the culture medium by an artificial cerebro-spinal fluid, constantly perfused at a rate of 1ml/min and containing (in mM): 145 NaCl, 4 KCl, 2 Na-pyruvate, 5 HEPES, 5 glucose, 2 $CaCl_2$, and 1 $MgCl_2$ (pH adjusted to 7.4 with NaOH). Voltage traces were sampled at 20 kHz, A/D converted at 16 bits, and stored on a personal computer employing the software LCG (Linaro et al., 2014). The same hardware/software system was employed to synthesize a variety of current-clamp stimulation waveforms, employed for estimating passive (i.e., membrane capacitance and input resistance) and active neuronal properties (i.e., rheobase current, frequency-current curve, spike-frequency adaptation index) of single cells. Recordings were analyzed off-line, employing custom scripts written in MATLAB (The MathWorks, Natick, US) or Excel (Microsoft, USA). The minor differences in AP's trajectory features (Fig. 2H, S3G) reflect the impact of hypoxia or DMOG on cell excitability (not significant).

Network-level extracellular recordings were performed in Neurobasal medium, supplemented with 1x B27 and 0.5 mM glutamine (Life Technologies). Across five distinct dissociation procedures, sister and non-sister cultures were plated on 28 multi-electrode arrays (MEAs). Hypoxic incubation was made in 1% O_2, 5% CO_2, and 94% N_2 atmosphere. The DMOG treatment was performed by adding it to the MEAs' bath at 1 mM final concentration. The described experiments were made overnight between DIV 13-14 and 20-21. Lentiviral transduction was accomplished by incubating overnight the neurons with 10 MOI particles. The electric network activity was recorded on all MEAs at DIV 13,14,15, and from DIV 20 to 22 only for hypoxia experiments. Electrophysiological recordings were performed by means MEA1060BC amplifiers, (Multichannel Systems GmBH, Reutlingen, Germany) inside an electronic friendly incubator, maintaining 37°C, 5% CO2, and 100% R.H. This allowed us to monitor simultaneously, chronically, and non-invasively the neuronal electrical activity from up to 59 locations within the very same culture. MEA recordings were analyzed off-line by QSpikeTools (Mahmud et al., 2014). Briefly, the extracellular electric fields were monitored from up to 59 independent electrodes in each MEAs, sampled at 25 kHz / channel, 1200x amplified, bandpass-filtered (400-3000Hz), and digitally recorded for 60 min every day. Elementary spike-sorting, only based on spike-shape peak polarity, was performed. Epochs of spontaneous synchronized firing across the MEAs electrodes were identified over 1 ms bins and by employing a threshold equal to 10. Neurons excitability in all MEAs was probed by low frequency (0.2 Hz) electrical extracellular stimulation, employing a stimulus isolator (STG1002, Multichannel Systems, Germany) programmed and driven by a custom made MATLAB (The MathWorks, USA). Four electrodes were chosen after probing 10 random sites of all electrodes. Stimuli were characterized by a square biphasic waveform of 1 ms duration and 1.6 V amplitude.

SUPPLEMENTAL REFERENCES

Aragones, J., Jones, D.R., Martin, S., San Juan, M.A., Alfranca, A., Vidal, F., Vara, A., Merida, I., and Landazuri, M.O. (2001). Evidence for the involvement of diacylglycerol kinase in the activation of hypoxia-inducible transcription factor 1 by low oxygen tension. J Biol Chem *276*, 10548-10555.

Arranz, A.M., Delbroek, L., Van Kolen, K., Guimaraes, M.R., Mandemakers, W., Daneels, G., Matta, S., Calafate, S., Shaban, H., Baatsen, P.*, et al.* (2015). LRRK2 functions in synaptic vesicle endocytosis through a kinase-dependent mechanism. J Cell Sci *128*, 541-552.

Attardo, A., Calegari, F., Haubensak, W., Wilsch-Brauninger, M., and Huttner, W.B. (2008). Live imaging at the onset of cortical neurogenesis reveals differential appearance of the neuronal phenotype in apical versus basal progenitor progeny. PLoS One *3*, e2388.

Goedhart, J., von Stetten, D., Noirclerc-Savoye, M., Lelimousin, M., Joosen, L., Hink, M.A., van Weeren, L., Gadella, T.W., Jr., and Royant, A. (2012). Structure-guided evolution of cyan fluorescent proteins towards a quantum yield of 93%. Nat Commun *3*, 751.

Haase, V.H., Glickman, J.N., Socolovsky, M., and Jaenisch, R. (2001). Vascular tumors in livers with targeted inactivation of the von Hippel-Lindau tumor suppressor. Proceedings of the National Academy of Sciences of the United States of America *98*, 1583-1588.

Hotulainen, P., Llano, O., Smirnov, S., Tanhuanpaa, K., Faix, J., Rivera, C., and Lappalainen, P. (2009). Defining mechanisms of actin polymerization and depolymerization during dendritic spine morphogenesis. J Cell Biol *185*, 323-339.

Iliopoulos, O., Kibel, A., Gray, S., and Kaelin, W.G., Jr. (1995). Tumour suppression by the human von Hippel-Lindau gene product. Nat Med *1*, 822-826.

Kayser, M.S., Nolt, M.J., and Dalva, M.B. (2008). EphB receptors couple dendritic filopodia motility to synapse formation. Neuron *59*, 56-69.

Leite de Oliveira, R., Deschoemaeker, S., Henze, A.T., Debackere, K., Finisguerra, V., Takeda, Y., Roncal, C., Dettori, D., Tack, E., Jonsson, Y.*, et al.* (2012). Gene-targeting of Phd2 improves tumor response to chemotherapy and prevents side-toxicity. Cancer cell *22*, 263-277.

Linaro, D., Couto, J., and Giugliano, M. (2014). Command-line cellular electrophysiology for conventional and real-time closed-loop experiments. J Neurosci Methods *230*, 5-19.

Livet, J., Weissman, T.A., Kang, H., Draft, R.W., Lu, J., Bennis, R.A., Sanes, J.R., and Lichtman, J.W. (2007). Transgenic strategies for combinatorial expression of fluorescent proteins in the nervous system. Nature *450*, 56-62.

Mahmud, M., Pulizzi, R., Vasilaki, E., and Giugliano, M. (2014). QSpike tools: a generic framework for parallel batch preprocessing of extracellular neuronal signals recorded by substrate microelectrode arrays. Front Neuroinform *8*, 26.

Marom, S., and Shahaf, G. (2002). Development, learning and memory in large random networks of cortical neurons: lessons beyond anatomy. Q Rev Biophys *35*, 63-87.

Niwa, H., Yamamura, K., and Miyazaki, J. (1991). Efficient selection for high-expression transfectants with a novel eukaryotic vector. Gene *108*, 193-199.

O'Gorman, S., Fox, D.T., and Wahl, G.M. (1991). Recombinase-mediated gene activation and site-specific integration in mammalian cells. Science *251*, 1351-1355.

Ruiz de Almodovar, C., Fabre, P.J., Knevels, E., Coulon, C., Segura, I., Haddick, P.C., Aerts, L., Delattin, N., Strasser, G., Oh, W.J*., et al.* (2011). VEGF mediates commissural axon chemoattraction through its receptor Flk1. Neuron *70*, 966-978.

Ryan, H.E., Poloni, M., McNulty, W., Elson, D., Gassmann, M., Arbeit, J.M., and Johnson, R.S. (2000). Hypoxia-inducible factor-1alpha is a positive factor in solid tumor growth. Cancer Res *60*, 4010-4015.

Shaner, N.C., Campbell, R.E., Steinbach, P.A., Giepmans, B.N., Palmer, A.E., and Tsien, R.Y. (2004). Improved monomeric red, orange and yellow fluorescent proteins derived from Discosoma sp. red fluorescent protein. Nat Biotechnol *22*, 1567-1572.

Sorra, K.E., and Harris, K.M. (2000). Overview on the structure, composition, function, development, and plasticity of hippocampal dendritic spines. Hippocampus *10*, 501-511.

Spiga, S., Acquas, E., Puddu, M.C., Mulas, G., Lintas, A., and Diana, M. (2011). Simultaneous Golgi-Cox and immunofluorescence using confocal microscopy. Brain Struct Funct *216*, 171-182.

Tronche, F., Kellendonk, C., Kretz, O., Gass, P., Anlag, K., Orban, P.C., Bock, R., Klein, R., and Schutz, G. (1999). Disruption of the glucocorticoid receptor gene in the nervous system results in reduced anxiety. Nature genetics *23*, 99-103.

Wilm, M., Shevchenko, A., Houthaeve, T., Breit, S., Schweigerer, L., Fotsis, T., and Mann, M. (1996). Femtomole sequencing of proteins from polyacrylamide gels by nano-electrospray mass spectrometry. Nature *379*, 466-469.

Woo, M.S., Ohta, Y., Rabinovitz, I., Stossel, T.P., and Blenis, J. (2004). Ribosomal S6 kinase (RSK) regulates phosphorylation of filamin A on an important regulatory site. Molecular and cellular biology *24*, 3025-3035.

Ziv, N.E., and Smith, S.J. (1996). Evidence for a role of dendritic filopodia in synaptogenesis and spine formation. Neuron *17*, 91-102.